Proceedings of 24th Conference
on Decision and Control
Ft. Lauderdale, FL • December 1985

RIGID BODY LOAD IDENTIFICATION FOR MANIPULATORS

Christopher G. Atkeson, Chae H. An, John M. Hollerbach

Artificial Intelligence Laboratory
Massachusetts Institute of Technology
545 Technology Square
Cambridge, Massachusetts 02139

Summary

A method for estimating the mass, the center of mass, and the moments of inertia of a rigid body load during general manipulator movement is presented. The algorithm is derived from the Newton-Euler equations and incorporates measurements of the force and torque from a wrist force/torque sensor and of the arm kinematics. The identification equations are linear in the desired unknown parameters, which are estimated by least squares. We have implemented this identification procedure on a PUMA 600 robot equipped with an RTI FS-B wrist force/torque sensor, and on the MIT Serial Link Direct Drive Arm equipped with a Barry Wright Company Astek wrist force/torque sensor.

1 Introduction

This paper presents a method of estimating all of the inertial parameters of a rigid body load using a wrist force/torque sensor: the mass, the moments of inertia, the location of its center of mass, and the object's orientation relative to a force sensing coordinate system. This procedure has three steps:

1. A Newton-Euler formulation for the rigid body load yields dynamics equations linear in the unknown inertial parameters, when the moment of inertia tensor is expressed about the wrist sensing force coordinate system origin.

2. These inertial parameters are then estimated using a least squares estimation algorithm.

3. The location of the load's center of mass, its orientation, and its principal moments of inertia can be recovered from the sensor referenced estimated parameters.

In principle, there are no restrictions on the movements used to do this load identification, except that if accurate estimation of all the parameters is desired the motion must be sufficiently rich (ie., occupy more than one orientation with respect to gravity and contain angular accelerations in several different directions) and sometimes special test movements must be used to get accurate estimates of moment of inertia parameters.

There are several applications for this load identification procedure. The accuracy of path following and general control quality of manipulators moving external loads can be improved by incorporating a model of the load into the controller, as the effective inertial parameters of the last link of the manipulator change with the load. The mass, the center of mass, and the moments of inertia constitute a complete set of inertial parameters for an object; in most cases, these parameters form a good description of the object, although they do not uniquely define it. The object may be completely unknown at first and an inertial description of the object may be generated as the robot picks up and moves the object. The robot may also be used in a verification process, in which the desired specification of the object is known and the manipulator examines the object to verify if it is within the tolerances. Recognition, finding the best match of a manipulated object to one among a set of known objects, may also be desired. Finally, the estimated location of the center of mass and the orientation of the principal axis can be used to verify that the manipulator has grasped the object in the desired manner.

A key feature of our approach is that it requires no special test or identification movements and therefore can continuously interpret wrist force and torque sensory data during any desired manipulation. Previous methods of load identification were restricted in their application. Paul (1981) described two methods of determining the mass of a load when the manipulator is at rest, one requiring the knowledge of joint torques and the other forces and torques at the wrist. The center of mass and the load moments of inertia were not identified.

Coiffet (1983) utilized joint torque sensing to estimate the mass and center of mass of a load for a robot at rest. Moments of inertia were estimated with special test motions, moving only one axis at a time or applying test torques. Because of the intervening link masses and domination of inertia by the mass moments, joint torque sensing is less accurate than wrist force-torque sensing.

Olsen and Bekey (1985) assumed full force-torque sensing at the wrist to identify the load without special test motions. Mukerjee (1984, 1985) developed an approach similar to ours, again allowing general motion during load identification. Nevertheless, neither paper simulated or experimentally implemented their procedures to verify the correctness of the equations or to determine the accuracy of estimation in the presence of noise and imperfect measurements.

Our algorithm requires measurements of the force and torque due to a load and measurements or estimates of the position, velocity, acceleration, orientation, angular velocity, and angular acceleration of the force sensing coordinate system. The algorithm can handle incomplete force and torque measurement by simply eliminating the equations containing missing measurements. The necessary kinematic data can be obtained from the joint angles and, if available, the joint velocities of the manipulator. The inertial parameters of a robot hand can be identified using this algorithm and then the predicted forces and torques due to the hand can be subtracted from the sensed forces and torques.

This inertial parameter estimation algorithm was implemented using a PUMA 600 robot equipped with an RTI FS-B wrist force/torque sensor, and on the MIT Serial Link Direct Drive Arm (DDA) equipped with a Barry Wright Company Astek FS6-120A-200 6-axis wrist force/torque sensor.

2 The Newton-Euler Approach To The Load Identification Problem

2.1 Deriving The Parameter Equation

To derive equations for estimating the unknown inertial parameters, the coordinate systems in Figure 1 are used to relate different coordinate frames and vectors. O is an inertial or base coordinate system,

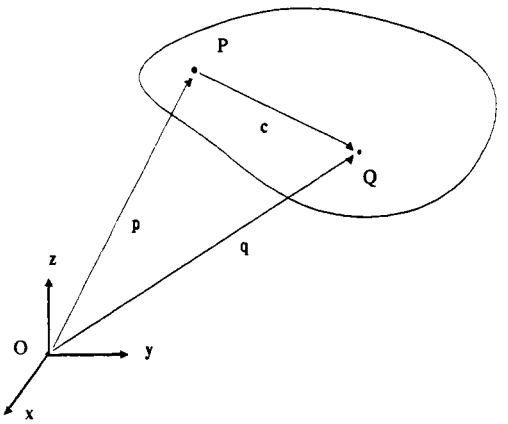

p: position vector from the origin of the base coordinate frame to the origin of the wrist sensor coordinate frame.

q: position vector from the origin of the base coordinate frame to the center of the mass of the load.

c: position vector from the origin of the wrist sensor coordinate frame to the center of the mass of the load.

Figure 1: Coordinate Frames.

which is fixed in space with gravity pointing along the $-z$ axis. $\mathbf{P}$ is the force reference coordinate system of a wrist force/torque sensor rigidly attached to the load. $\mathbf{Q}$ represents the principal axis of the rigid body load located at the center of mass. The x axis of $\mathbf{Q}$ is along the largest principal moment of inertia, and the z axis along the smallest. $\mathbf{Q}$ is unique up to a reflection in bodies with 3 distinct principal moments of inertia. In the derivation that follows all vectors are initially expressed in the base coordinate system $\mathbf{O}$.

The mass, moments of inertia, location of the center of mass, and orientation of the body (a rotation ${}_{Q}{}_{P}\mathbf{R}$ from the principal axes to the force reference system) are related to the motion of the load and the forces and torques exerted on it by the Newton-Euler equations. The net force ${}_{q}\mathbf{f}$ and the net torque ${}_{q}\mathbf{n}$ acting on the load at the center of mass are:

$$ {}_{q}\mathbf{f} = \mathbf{f} + m\mathbf{g} = m\ddot{\mathbf{q}} \tag{1} $$

$$ {}_{q}\mathbf{n} = \mathbf{n} - \mathbf{c} \times \mathbf{f} = {}_{q}\mathbf{I}\dot{\omega} + \omega \times ({}_{q}\mathbf{I}\omega) \tag{2} $$

where:

- $\mathbf{f}$ = the force exerted by the wrist sensor on the load at the point $\mathbf{p}$,
- m = the mass of the load,
- $\mathbf{g}$ = the gravity vector ($\mathbf{g} = [0, 0, -9.8\,\text{meters/sec}^2]$),
- $\ddot{\mathbf{q}}$ = the acceleration of the center of mass of the load,
- $\mathbf{n}$ = the torque exerted by the wrist sensor on the load at the point $\mathbf{p}$,
- $\mathbf{c}$ = the unknown location of the center of mass relative to the force sensing wrist origin $\mathbf{P}$,
- ${}_{q}\mathbf{I}$ = the moment of inertia tensor about the center of mass,
- ω = the angular velocity vector, and
- $\dot{\omega}$ = the angular acceleration vector.

We need to express the force and torque measured by the wrist sensor in terms of the product of known geometric parameters and the unknown inertial parameters. Although the location of the center of mass and hence its acceleration $\ddot{\mathbf{q}}$ are unknown, $\ddot{\mathbf{q}}$ is related to the the acceleration of the force reference frame $\ddot{\mathbf{p}}$ by

$$ \ddot{\mathbf{q}} = \ddot{\mathbf{p}} + \dot{\omega} \times \mathbf{c} + \omega \times (\omega \times \mathbf{c}) \qquad (3\,[7.40]^{1}) $$

Substituting (3) into (1),

$$ \mathbf{f} = m\ddot{\mathbf{p}} - m\mathbf{g} + \dot{\omega} \times m\mathbf{c} + \omega \times (\omega \times m\mathbf{c}) \tag{4} $$

Substituting (4) into (2),

$$ \mathbf{n} = {}_{q}\mathbf{I}\dot{\omega} + \omega \times ({}_{q}\mathbf{I}\omega) + m\mathbf{c} \times (\dot{\omega} \times \mathbf{c}) + m\mathbf{c} \times (\omega \times (\omega \times \mathbf{c})) + m\mathbf{c} \times \ddot{\mathbf{p}} - m\mathbf{c} \times \mathbf{g} \tag{5} $$

Although the terms $\mathbf{c} \times (\dot{\omega} \times \mathbf{c})$ and $\mathbf{c} \times (\omega \times (\omega \times \mathbf{c}))$ are quadratic in the unknown location of the center of mass $\mathbf{c}$, these quadratic terms are eliminated by expressing the moment of inertia tensor about the force sensor coordinate origin (${}_{p}\mathbf{I}$) instead of about the center of mass (${}_{q}\mathbf{I}$). Rewriting (5) as:

$$ \mathbf{n} = {}_{q}\mathbf{I}\dot{\omega} + \omega \times ({}_{q}\mathbf{I}\omega) + m[(\mathbf{c}^{T}\mathbf{c})\mathbf{1} - (\mathbf{c}\mathbf{c}^{T})]\dot{\omega} + \omega \times (m[(\mathbf{c}^{T}\mathbf{c})\mathbf{1} - (\mathbf{c}\mathbf{c}^{T})]\omega) + m\mathbf{c} \times \ddot{\mathbf{p}} - m\mathbf{c} \times \mathbf{g} \tag{6} $$

and using the three dimensional version of the parallel axis theorem

$$ {}_{p}\mathbf{I} = {}_{q}\mathbf{I} + m[(\mathbf{c}^{T}\mathbf{c})\mathbf{1} - (\mathbf{c}\mathbf{c}^{T})] \qquad (7\,[10.147]). $$

to simplify it results in:

$$ \mathbf{n} = {}_{p}\mathbf{I}\dot{\omega} + \omega \times ({}_{p}\mathbf{I}\omega) + m\mathbf{c} \times \ddot{\mathbf{p}} - m\mathbf{c} \times \mathbf{g} \tag{8} $$

($\mathbf{1}$ is the 3 dimensional identity matrix). We now express all the vectors in the wrist sensor coordinate system $\mathbf{P}$, since then the quantities $\mathbf{c}$ and ${}_{p}\mathbf{I}$ are constant. Moreover, the wrist force/torque sensor measures forces and torques directly in the $\mathbf{P}$ coordinate frame.

In order to formulate the above equations as a system of linear equations, the following equalities and notations are used:

$$ \omega \times \mathbf{c} = \begin{bmatrix} 0 & -\omega_x & \omega_y \\ \omega_z & 0 & -\omega_x \\ -\omega_y & \omega_x & 0 \end{bmatrix} \begin{bmatrix} c_x \\ c_y \\ c_z \end{bmatrix} \triangleq [\omega\times]\,\mathbf{c} \tag{9} $$

$$ \mathbf{I}\omega = \begin{bmatrix} \omega_x & \omega_y & \omega_z & 0 & 0 & 0 \\ 0 & \omega_x & 0 & \omega_y & \omega_z & 0 \\ 0 & 0 & \omega_x & 0 & \omega_y & \omega_z \end{bmatrix} \begin{bmatrix} I_{11} \\ I_{12} \\ I_{13} \\ I_{22} \\ I_{23} \\ I_{33} \end{bmatrix} \triangleq [\bullet\omega] \begin{bmatrix} I_{11} \\ I_{12} \\ I_{13} \\ I_{22} \\ I_{23} \\ I_{33} \end{bmatrix} \tag{10} $$

where

$$ \mathbf{I} = \mathbf{I}^{T} = \begin{bmatrix} I_{11} & I_{12} & I_{13} \\ I_{12} & I_{22} & I_{23} \\ I_{13} & I_{23} & I_{33} \end{bmatrix} \tag{11} $$

Using these expressions, Eqs. (4) and (8) can be written as a single matrix equation in the wrist sensor coordinate frame:

$$ \begin{bmatrix} f_x \\ f_y \\ f_z \\ n_x \\ n_y \\ n_z \end{bmatrix} = \begin{bmatrix} \ddot{\mathbf{p}} - \mathbf{g} & [\dot{\omega}\times] + [\omega\times][\omega\times] & \mathbf{0} \\ \mathbf{0} & [(\mathbf{g} - \ddot{\mathbf{p}})\times] & [\bullet\dot{\omega}] + [\omega\times][\bullet\omega] \end{bmatrix} \begin{bmatrix} m \\ mc_x \\ mc_y \\ mc_z \\ I_{11} \\ I_{12} \\ I_{13} \\ I_{22} \\ I_{23} \\ I_{33} \end{bmatrix} \tag{12} $$

or more compactly,

$$ \boldsymbol{w} = \boldsymbol{A}\boldsymbol{\phi} \tag{13} $$

where $\boldsymbol{w}$ is a 6 element wrench vector combining both the force and torque vectors, $\boldsymbol{A}$ is a 6×10 matrix and $\boldsymbol{\phi}$ is the vector of the 10

[1] Equation numbers in brackets refer to equations in Symon, 1971.

unknown inertial parameters. Note that the center of mass cannot be determined directly, but only as the mass moment mc. But since the mass m is separately determined, its contribution can be factored from the mass moment later.

2.2 Estimating The Parameters

The quantities inside the $\boldsymbol{A}$ matrix are computed by direct kinematics computation (Luh, Walker, and Paul, 1980) from the measured joint angles. The elements of the $\mathbf{w}$ vector are measured directly by the wrist force sensor. Since (13) represents 6 equations and 10 unknowns, at least two data points are necessary to solve for the ϕ vector, i.e. the force and the position data sampled at two different configurations of the manipulator. For robust estimates in the presence of noise, we actually need to use a larger number of data points. Each data point adds 6 more equations, whereas the number of unknowns, the elements of ϕ, remain constant. This can be represented by augmenting $\mathbf{w}$ and $\boldsymbol{A}$ as:

$$\mathbf{A} = \begin{bmatrix} \boldsymbol{A}[1] \\ \cdot \\ \cdot \\ \boldsymbol{A}[n] \end{bmatrix}, \qquad \mathbf{w} = \begin{bmatrix} \mathbf{w}[1] \\ \cdot \\ \cdot \\ \mathbf{w}[n] \end{bmatrix}, \qquad n = \text{number of data points} \tag{14}$$

where each $\boldsymbol{A}[i]$ and $\mathbf{w}[i]$ are matrix and vector quantities described in (12). Formulated this way, any linear estimation algorithm can be used to identify the ϕ vector. A simple and popular method is the least squares method. The estimate for ϕ is given by:

$$\hat{\phi} = (\mathbf{A}^T\mathbf{A})^{-1}\mathbf{A}^T\mathbf{w} \tag{15}$$

Equation (15) can also be formulated in a recursive form (Ljung, 1983) for on-line estimation.

2.3 Recovering Object And Grip Parameters

The estimated inertial parameters (m, mc, ${}_P\mathrm{I}$) are adequate for control, but for object recognition and verification we also require the principal moments of inertia I_1, I_2, I_3, the location of the center of mass $\mathbf{c}$, and the orientation ${}_{Q}{}_{P}\mathbf{R}$ of $\mathbf{Q}$ with respect to $\mathbf{P}$.

The parallel axis theorem is used to compute the inertia terms translated to the center of mass of the load.

$$\hat{\mathbf{c}} = \frac{\widehat{mc}}{\hat{m}} \tag{16}$$

$${}_{q}\hat{\mathbf{I}} = {}_{P}\hat{\mathbf{I}} - \hat{m}[(\hat{\mathbf{c}}^T\hat{\mathbf{c}})\mathbf{1} - (\hat{\mathbf{c}}\hat{\mathbf{c}}^T)] \tag{17}$$

The principal moments are obtained by diagonalizing ${}_{q}\hat{\mathbf{I}}$.

$${}_{q}\hat{\mathbf{I}} = {}_{Q}{}_{P}\hat{\mathbf{R}} \begin{bmatrix} \hat{I}_1 & 0 & 0 \\ 0 & \hat{I}_2 & 0 \\ 0 & 0 & \hat{I}_3 \end{bmatrix} {}_{Q}{}_{P}\hat{\mathbf{R}}^T \tag{18}$$

This diagonalization can always be achieved since ${}_{q}\hat{\mathbf{I}}$ is symmetric, but when two or more principal moments are equal the rotation matrix ${}_{Q}{}_{P}\mathbf{R}$ is no longer unique.

3 Experimental Results

3.1 Estimation on the PUMA Robot

The inertial parameter estimation algorithm was originally implemented on a PUMA 600 robot equipped with an RTI FS-B wrist force/torque sensor (Figure 2), which measures all six forces and torques. The PUMA 600 has encoders at each joint to measure joint angles, but no tachometers. Thus, to obtain the joint velocities and accelerations, the joint angles are differentiated and double-differentiated, respectively, by a digital differentiating filter (Figure 3). The cutoff frequency of 33 Hz for the filter was determined empirically to produce the best results. Both the encoder data and

Figure 2: Puma with a test load.

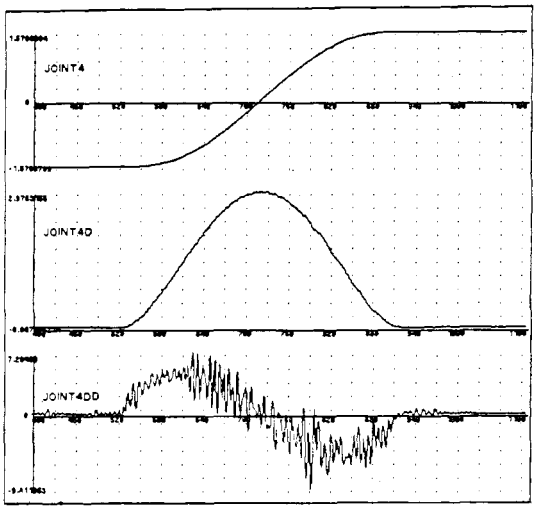

Figure 3: Measured angle θ, calculated angular velocity $\dot{\theta}$, and calculated angular acceleration $\ddot{\theta}$ for joint 4.

the wrist sensor data were initially sampled at 1000 Hz. It was later determined that a sampling rate of 200 Hz was sufficient, and the data were resampled at the lower rate to reduce processing time. A least squares identification algorithm was implemented as an off-line computation, but an on-line implementation would have been straightforward.

3.1.1 Static Estimation Using The PUMA

To test the calibration of the force sensor and the kinematics of the PUMA arm a static identification was performed. The forces and torques are now due only to the gravity acting on the load, and equations (4) and (8) simplify to

$$\mathbf{f} = -m\mathbf{g} \tag{19}$$

$$\mathbf{n} = -m\mathbf{c} \times \mathbf{g} \tag{20}$$

As seen in (19) and (20), only the mass and the center of mass can be identified while the manipulator is stationary.

To avoid needing to determine the gripper geometric parameters, the center of mass estimates are evaluated by the estimates of the

Parameters	*Actual Values*	*Static Estimates*	*Dynamic Estimates*
Mass (kg)	1.106	1.103	1.067
Change in $c_y(m)$	0.037	0.037	0.039
Mass (kg)	1.106	1.107	1.084
Change in $c_y(m)$	-0.043	-0.043	-0.042
Mass (kg)	1.106	1.100	1.073
Change in $c_y(m)$	-0.021	-0.020	-0.021
Mass (kg)	1.106	1.099	1.074
Change in $c_y(m)$	0.018	0.018	0.020

Table 1: Mass and the Center of Mass Estimates

Parameters ($kg \cdot m^2$)	*Actual Values*	PUMA[1] *Estimates*	PUMA[2] *Estimates*	DDA[1] *Estimates*
I_{11}	0.0244	0.0192	0.0246	0.0233
I_{12}	0	-0.0048	0.0006	0.0003
I_{13}	0	0.0019	0.0008	0.0007
I_{22}	0.0007	0.0021	0.0036	0.0001
I_{23}	0	-0.0016	-0.0004	-0.0002
I_{33}	0.0242	0.0176	0.0199	0.0236

[1] (all joints moving)
[2] (3 special test movements combined)

Table 2: Estimates of the moments of inertia

changes in the center of mass as the load is moved along the y-axis from the reference position by known amounts. The results of estimation are shown in the third column of Table 1 for an aluminum block ($2 \times 2 \times 6in.$) with a mass of $1.106Kg$. Only the changes in c_y are shown in Table 1; the estimates of c_x and c_z remained within $1mm$ of the reference values ($c_x = 1mm$ and $c_z = 47mm$). Each set of estimates were computed from 6 sets of data, i.e. data taken at 6 different positions and orientations of the manipulator, where each data point is averaged over 1000 samples to minimize the effects of noise. The results show that in the static case the mass of the load can be estimated to within $10g$ of the actual mass. The center of mass can be estimated to within $1mm$ of the actual values for this load.

Static load estimation only tests the force sensor calibration and the position measurement capabilities of the robot on which the sensor is mounted. In order to assess the effects of the dynamic capabilites of the robot on load estimation and to be able to estimate the moments of inertia of the load we must assess parameter estimation during general movement.

3.1.2 Dynamic Estimation Using The PUMA

In the dynamic case, the joint position encoder and the wrist sensor data are sampled while the manipulator is in motion. A fifth order polynomial trajectory in joint space was used to minimize the mechanical vibrations at the beginning and the end of the movement, and to improve the signal to noise ratio (SNR) in the acceleration data (Figure 3). For more popular bang-coast-bang type trajectories, the joint accelerations are zero except at the beginning and the end of the movements, resulting in poor SNR in the acceleration data for most of the movement.

We found that the PUMA robot lacked the acceleration capacity necessary to estimate the moments of inertia of the load. It also lacked true velocity sensors at the joints, which made estimation of the acceleration of the load difficult. The dynamic estimates of mass and center of mass for the previous load are shown in the last column of Table 1. The data used in these estimates were sampled while the manipulator was moving from $[0,0,0,-90,0,0]$ to $[90,-60,90,90,90,90]$ degrees on a straight line in joint space in 2 seconds. Joint 4 of the PUMA has a higher maximum acceleration than the other joints, and thus, a longer path was given for it. This movement was the fastest the PUMA can execute using the fifth order trajectory without reaching the maximum acceleration for any of its joints. The estimates used all 400 data points sampled during the 2 second movement. The results show slight deterioration in these estimates when compared to the static estimates; but they are still within $40g$ and $2mm$ of the actual mass and displacement, respectively. However, the SNR in the acceleration and the force/torque data were too low for accurate estimates of the moments of inertia for this load ($0.00238Kg \cdot m^2$ in the largest principal moment). In this case, the torque due to gravity is approximately 40 times greater than the torque due to the maximum angular acceleration of the load. Thus, even slight noise in the data would result in poor estimates of **I**.

3.1.3 Special Test Movements Using The PUMA

Therefore, experiments with a different load were performed for the estimates of the moments of inertia. The new experimental load is shown in Figure 2. This load has large masses at the two ends of the aluminum bar, resulting in large moments of inertia in two directions ($\sim 0.024kg \cdot m^2$) and a small moment in the other. A typical set of estimates of the moments of inertia at the center of mass frame for the load with the gripper subtracted out are shown in Table 2 for the above all-joints-moving trajectory. They contain some errors but are fairly close to the actual values.

In order to improve the estimates, the data were sampled while the robot was following three separate 2-second rotational trajectories around the principal axes of the load. Such trajectories used joint 4 and joint 6 only, and resulted in higher acceleration data than the previous trajectory, thus improving the SNR in both the acceleration and the force/torque data. Typical estimates for these special movements show improvements over the estimates with the previous trajectory (Table 2). Although the estimate of I_{22} is slightly worse than before, all the other terms have improved; the cross terms, especially, are much smaller than before. However, these estimates of **I** are not as accurate as the estimates of the mass and the center of mass shown in Table 1. Most of the error is probably due to the large amount of noise present in the acceleration data caused by differentiating the joint angle data twice. Part of the error may be due to inaccuracies in the current kinematic parameters of the manipulator. Experiments have shown that the actual orientation of the robot can be up to 4° off from the orientation computed from the encoder data.

Figure 4 shows the comparison of the measured forces and torques, and the computed forces and torques from the estimated parameters and the measured joint data using the simulator for the original trajectory. The two sets of figures match very well even in the mechanical vibrations, verifying qualitatively the accuracy of the estimates. This suggests that for control purposes even poor estimation of moment of inertia parameters will allow good estimates of the total force and torque necessary to achieve a trajectory. This makes good sense in that the load forces with the PUMA are dominated by gravitational componenents, and angular accelerations experienced by the load are small relative to those components.

The effect of the errors causing poor estimates of moment of inertia parameters could be alleviated by increasing the angular acceleration experienced by the load. Since we had reached the sustained acceleration capacity of even an unloaded PUMA robot, we decided to explore this issue using the MIT Serial Link Direct Drive Arm. This robot can achieve higher sustained accelerations than the PUMA and in addition is also equipped with tachometers at the joints, making estimation of acceleration much easier.

3.2 The MIT Serial Link Direct Drive Arm

The inertial parameter estimation algorithm was next implemented on the MIT Serial Link Direct Drive Arm (DDA), equipped with a Barry Wright Company Astek FS6-120A-200 6-axis force/torque sensor which again measures all three forces and three torques about

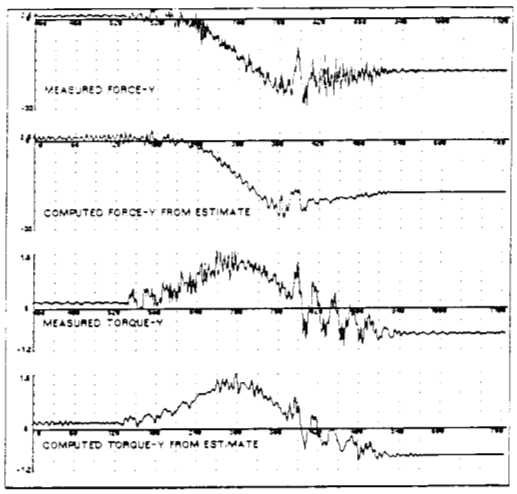

Figure 4: Measured force/torque data and computed force/torque data from the estimates using the PUMA.

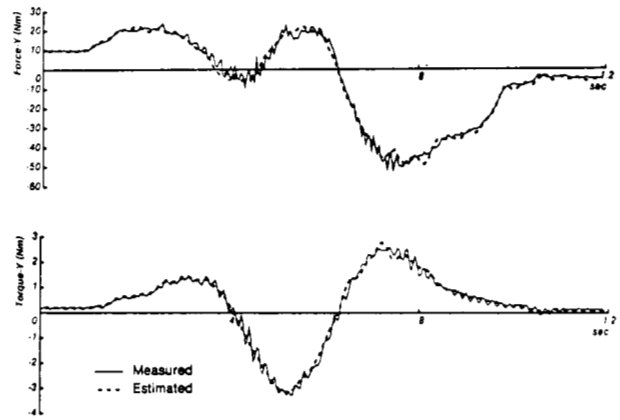

Figure 5: Measured force/torque data and computed force/torque data from the estimates using the Direct Drive Arm.

a point. The DDA is described in An, Atkeson, Hollerbach (1985), and is capable of higher tip velocities and accelerations than the PUMA. The DDA has tachometers on each of its three joints so that numerical differentiation of positions is unnecessary, but we still had to digitally differentiate the velocities to find the accelerations using a cutoff frequency of 30Hz. The positions and velocities of the robot were initially sampled at 1kHz but were later down-sampled to match the sampling frequency of the force/torque sensor of 240 Hz. The identification procedure was again implemented off-line.

3.2.1 Dynamic Estimation Using The Direct Drive Arm

The data used for estimating the inertial parameters of the load were sampled while the manipulator was moving from $(280, 269.1, -30)$ to $(80, 19.1, 220)$ in one second. Again a fifth order polynomial straight line trajectory in joint space was used. The resulting estimates for the moment of inertia parameters are shown in the last column of Table 2. The estimates for the mass and the location of the center of mass were as good as the PUMA results and are not shown. We see that the moment of inertia parameters estimated are on the whole better than the PUMA results.

Parameters estimated for a set of special test movements using the Direct Drive Arm were not substantially different. Our special test movements for the DDA were not substantially faster than the movement of all joints, and thus probably contained the same amount of information.

Finally, Figure 5 shows the comparison of typical measured forces and torques with computed forces and torques from the estimated parameters and the measured joint data using the simulator for the original trajectory. Once again we have a very good match between the measured and predicted forces and torques. Thus we see that the combination of higher angular accelerations and good velocity sensing results in better parameter estimates, as hoped.

4 Discussion

4.1 Did The Algorithm Work?

This paper describes an attempt to characterize the usefulness of wrist force/torque sensing for estimating the inertial parameters of rigid body loads for control and recognition/verification/grasping. Our conclusion is that prediction of forces for control can be good and seems to work well in our implementations. Identifying parameters well enough for recognition of the object may require large accelerations or special test movements in order to accurately identify the moment of inertia parameters.

It is important to realize that there are two distinct uses of an identified model. For control what matters is matching the input-output behavior of the model (in this case the relationship of load trajectory to load forces and torques) to reality, while for recognition/verification what matters is matching estimated parameters to a set of parameters postulated for reality. We find that both of our implementations of load inertial parameter estimation successfully match the input output behavior of the load (see Figures 4 and 5), although we have not yet used this information in a control scheme. However, we find that the limited acceleration capacity of the PUMA robot and its limited sensing do not permit us to estimate the moments of inertia of the load accurately without the use of special test motions. In all cases the mass and the location of the center of mass could be accurately estimated from both series of static measurements, and dynamic measurements.

This work is preliminary in that an adequate statistical characterization of the errors of the estimated parameters of the predicted forces has not been attempted. Nevertheless, we have gained insight into the sources of such errors.

4.2 Sources of Error

The ultimate source of error is the random noise inherent in the sensing process itself. The noise levels on the position and velocity sensing are probably negligible, and could be further reduced by appropriate filtering using a model based filter such as the Extended Kalman Filter. The force and torque measurement process involve measuring strain of structure members in the sensor with semiconductor strain gages. The random noise involved in such measurements is also probably negligible.

4.2.1 Bias Errors

However, semiconductor strain gages are notoriously prone to drift. We feel that periodic recalibration of the offsets (very often) and the strain to force calibration matrix (often) may be necessary to reduce load parameter estimation errors further. Before using the force sensors we allowed the system to warm up and we recalibrated the offsets before each data collection session and checked for a change in the calibrated offsets afterward.

4.2.2 Unmodelled Dynamics

A further source of noise is unmodelled structural dynamics. Neither the robot links nor the load itself are perfectly rigid bodies. A greater source of concern is the compliance of the force sensor itself. In order to generate structural strains large enough to be reliably measured

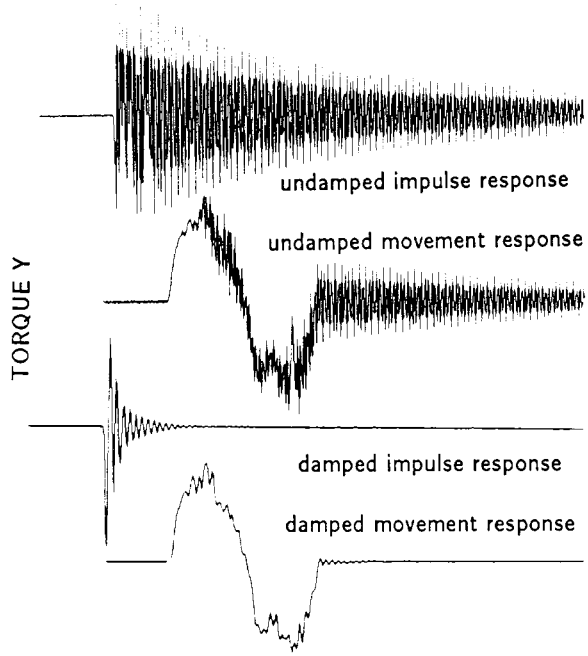

Figure 6: Vibration of load on force sensor.

with even semiconductor strain gage technology, a good deal of compliance is introduced into the force sensor. The load rigidly attached to the force sensor becomes a relatively undamped spring mass system. The response of the Astek force sensor to a tap on an attached load is shown in the "undamped impulse response" record of Figure 6. The effect of robot movement on this spring mass system is shown in the "undamped movement response" record.

There are several approaches to take to deal with this problem of unmodelled dynamics. One approach is to attempt to identify the additional dynamics. This greatly increases the complexity of the identification process and the amount of data that needs to be collected to get reliable estimates of any parameter. We feel such an approach should only be taken as a last resort.

Another approach is to try to avoid exciting the unmodelled dynamics by choosing robot trajectories that were as smooth as possible. This is one reason why we chose 5th order polynomial trajectories, so that we could maintain continuity of velocities and accelerations. Using higher order polynomials would result in even greater smoothness. However, we found that with the PUMA a smooth commanded trajectory did not result in a smooth actual trajectory, in that the control methods used and the actual hardware of the robot still introduced substantial vibration. One way to tell if the PUMA is turned on is to touch it and feel if it is vibrating. Vibrations were less of a problem with the Direct Drive Arm, althought still present.

The most successful approach is to mechanically damp out the vibrations by introducing some form of energy dissipation into the structure. We added hard rubber washers between the force sensor and the load, and the "damped impulse response" of Figure 6 illustrates the response of the force sensor to a tap on the load. We see that the oscillations decay much faster. The "damped movement response" indicates that this mechanical damping greatly reduces the effect of movement on the resonant modes of the force sensor plus load. The conclusion we draw is that appropriate damping should be built into force sensors, just as accelerometers are filled with oil to provide a critically damped response for a specified measurement bandwidth. Failing that, energy dissipation must be introduced either into the structural components of the robot or into the gripper either structurally or as a viscous skin. Appropriate mechanical damping may also be useful when using a force sensor in closed loop force control.

4.2.3 Optimal Filtering

Finally, the need to numerically differentiate the velocity to find the acceleration greatly amplifies whatever noise is present. One can avoid the need to explicitly calculate acceleration by integrating equations (4) and (8). However, we feel that an effort to characterize the various noise sources and an attempt to "optimally" filter and differentiate/integrate the data will result in better estimates. We are presently investigating such an approach.

4.3 Why Estimating Moment of Inertia Parameters is Hard

One of the factors that make it difficult to accurately identify moments of inertia is the typically large contribution of gravitational torque, which depends only on the mass and the relative location of the center of mass to the force sensing coordinate origin. A point mass rotated at a radius of $5cm$ from a horizontal axis must complete a full 360° rotation in 425 milliseconds for the torque due to angular acceleration to be equal to the gravitational torque, if a 5th order polynomial trajectory is used. A way to avoid gravitational torques is to rotate the load about vertical axis, or to have the point of force/torque sensing close to the center of mass.

A simple example will illustrate the difficulty of recovering principle moments of inertia, given the moment of inertia tensor about the force sensing origin. The principle moment of inertia of a uniform sphere surface is only 2/7 of the total moment of inertia when it is rotated about an axis tangent to its surface, so that the effects of any errors in estimating the mass, the location of the center of mass, and the grip moments of inertia are amplified when the principle moment of inertia is calculated. This problem can be reduced by having the point of force sensing as close to the center of mass as possible

It still may be difficult to find the orientation of the principle moments of inertia even when the moment of inertia tensor about the center of mass has been estimated fairly accurately. This occurs when two or more principle moments of inertia are approximately equal. Finding the orientation of the principle axis is equivalent to diagonalizing a symmetric matrix, which becomes ill-conditioned when some of the eigenvalues are almost equal. A two dimensional example that illustrates the problem. Consider the diagonalized matrix

$$\begin{bmatrix} \cos(\theta) & -\sin(\theta) \\ \sin(\theta) & \cos(\theta) \end{bmatrix} \begin{bmatrix} \lambda_1 & 0 \\ 0 & \lambda_2 \end{bmatrix} \begin{bmatrix} \cos(\theta) & \sin(\theta) \\ -\sin(\theta) & \cos(\theta) \end{bmatrix} \tag{21}$$

with eigenvalues $\{\lambda_1, \lambda_2\}$ and whose first principle axis is oriented at an angle θ with respect to the x axis. When the two eigenvalues are almost equal, the terms of the matrix dependent on the angle θ become very small. By substituting $\lambda_1 - \lambda_2 = \epsilon$ into the matrix (21),

$$\begin{bmatrix} \lambda_2 + \epsilon\cos^2(\theta) & \epsilon\cos(\theta)\sin(\theta) \\ \epsilon\cos(\theta)\sin(\theta) & \lambda_2 + \epsilon\sin^2(\theta) \end{bmatrix} \tag{22}$$

All terms that contain angle information are multiplied by the difference (ϵ) of the principle moments of inertia. With a fixed amount of noise in each of the entries of the identified moment of inertia matrix, the orientation of the principle axis (θ) will become more and more difficult to recover.

Acknowledgment

This paper describes research done at the Artificial Intelligence Laboratory of the Massachusetts Institute of Technology. Support for the laboratory's artificial intelligence research is provided in part by the Systems Development Foundation and the Defense Advanced Research Projects Agency under Office of Naval Research contracts N00014-80-C-050 and N00014-82-K-0334. Partial support for C. Atkeson was provided by a Whitaker Fund Graduate Fellowship and an NSF Graduate Fellowship, for C. An by an NSF Graduate Fellowship, and for J. Hollerbach by an NSF Presidential Young Investigator

Award.

References

Asada, H., and Youcef-Toumi, K. 1984. Analysis and design of a direct-drive arm with a five-bar-link parallel drive mechanism. *ASME J. Dynamic Systems, Meas., Control.* 106: 225-230.

An, C., Atkeson, C. and Hollerbach, J. 1985 (December 11-13). Estimation of Inertial Parameters of Rigid Body Links of Manipulators. *Proc 24th Conf. Decision and Control.* Fort Lauderdale, Florida:.

Coiffet, P. 1983. *Robot Technology: Interaction With The Environment.* 2 Englewood Cliffs, NJ: Prentice-Hall, Inc..

Ljung, L. and Soderstrom, T. 1983. *Theory and Practice of Recursive Idenfication.* MIT Press.

Luh, J.Y.S., Walker, M., and Paul, R.P. 1980. On-line computational scheme for mechanical manipulators. *J. Dynamic Systems, Meas., Control.* 102: 69-76.

Mukerjee, A. 1984 (November). Adaptation in biological sensory-motor systems: A model for robotic control. *Proc., SPIE Conf. on Intelligent Robots and Computer Vision, SPIE Vol. 521.* Cambridge:.

Mukerjee, A., and Ballard, D.H. 1985 (Mar. 25-28). Self-calibration in robot manipulators. *Proc. IEEE Conf. Robotics and Automation.* St. Louis: pp. 1050-1057.

Olsen, H.B., and Bekey, G.A. 1985 (Mar. 25-28). Identification of parameters in models of robots with rotary joints. *Proc. IEEE Conf. Robotics and Automation.* St. Louis: pp. 1045-1050.

Paul, R.P. 1981. *Robot Manipulators: Mathematics, Programming, and Control.* Cambridge, Mass.: MIT Press.

Symon, K.R. 1971. *Mechanics.* Reading, Mass.: Addison-Wesley.

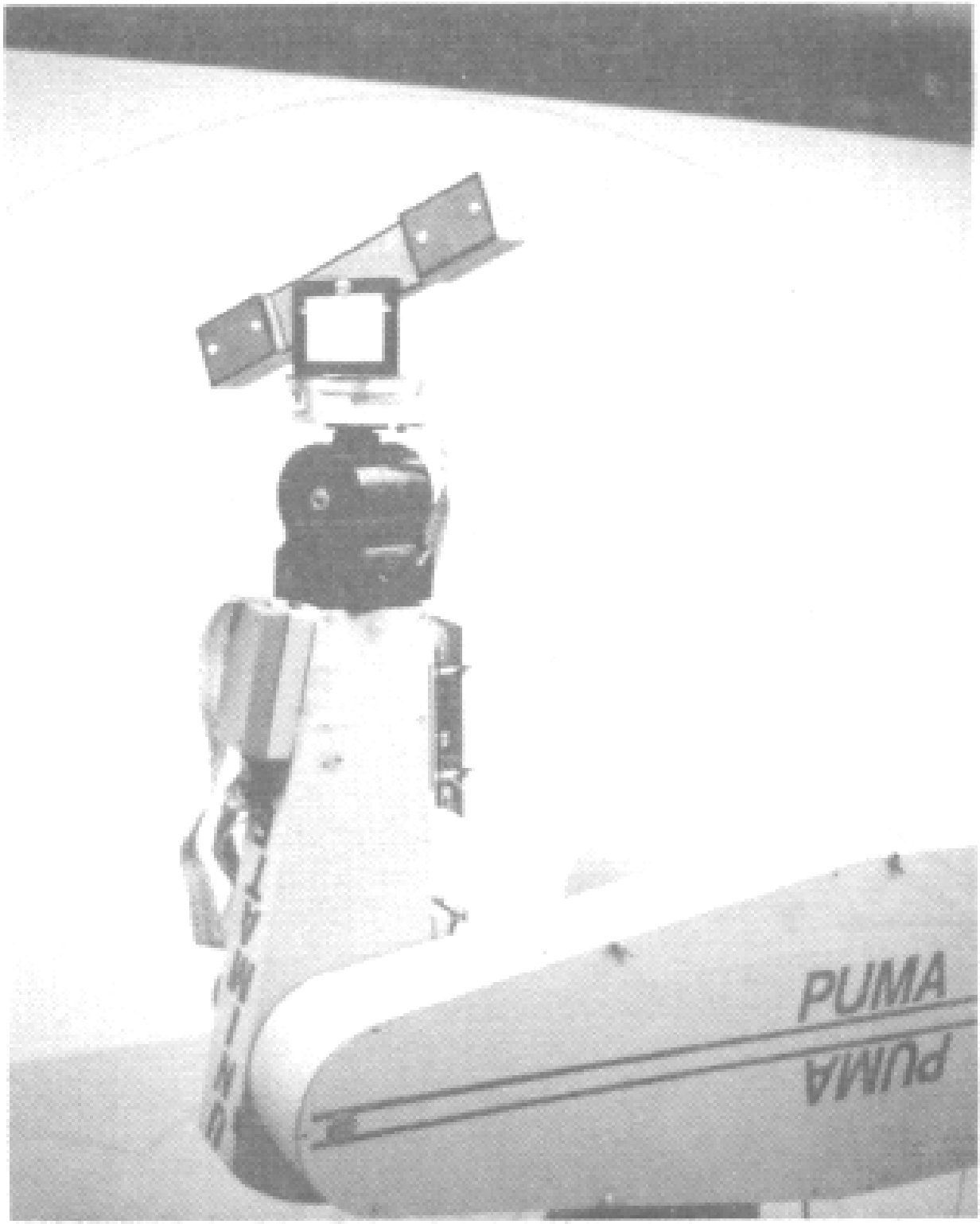

Figure 2: Puma with a test load.